

Cosmology from MAXIMA-1, BOOMERANG & COBE/DMR CMB Observations.

A.H. Jaffe,^{1,2,3} P.A.R. Ade,⁴ A. Balbi,^{1,5,6} J.J. Bock,⁷ J.R. Bond,⁸ J. Borrill,^{1,2,3,9} A. Boscaleri,¹⁰ K. Coble,¹¹ B.P. Crill,¹² P. de Bernardis,¹³ P. Farese,¹¹ P.G. Ferreira,^{14,15} K. Ganga,^{12,16} M. Giacometti,¹³ S. Hanany,^{17,1} E. Hivon,^{1,12} V.V. Hristov,¹² A. Iacoangeli,¹³ A.E. Lange,^{1,12} A.T. Lee,^{1,2} L. Martinis,¹⁸ S. Masi,¹³ P.D. Mauskopf,¹⁹ A. Melchiorri,¹³ T. Montroy,¹¹ C.B. Netterfield,²⁰ S. Oh,^{1,21} E. Pascale,¹⁰ F. Piacentini,¹³ D. Pogosyan,⁸ S. Prunet,⁸ B. Rabii,^{1,2,21} S. Rao,²² P.L. Richards,^{1,21} G. Romeo,²² J.E. Ruhl,^{1,11} F. Scaramuzzi,¹⁸ D. Sforna,¹³ G.F. Smoot,^{1,2,21,23} R. Stompor,^{1,2,24} C.D. Winant,^{1,2,21} and J.H.P. Wu³

¹*Center for Particle Astrophysics, University of California, Berkeley, CA 94720*

²*Space Sciences Laboratory, University of California, Berkeley, CA 94720*

³*Department of Astronomy, University of California, Berkeley, CA 94720*

⁴*Queen Mary and Westfield College, London, UK*

⁵*Dipartimento di Fisica, Università Tor Vergata, Roma, Italy*

⁶*Division of Physics, Lawrence Berkeley National Laboratory, Berkeley, CA 94720*

⁷*Jet Propulsion Laboratory, Pasadena, CA 91109*

⁸*Canadian Institute for Theoretical Astrophysics, University of Toronto, Toronto M5S 3H8, Canada*

⁹*National Energy Research Scientific Computing Center, LBNL, Berkeley, CA 94720*

¹⁰*IROE-CNR, Firenze, Italy*

¹¹*Department of Physics, University of California, Santa Barbara, CA 93106*

¹²*California Institute of Technology, Pasadena, CA 91125*

¹³*Dipartimento di Fisica, Università La Sapienza, Roma, Italy*

¹⁴*Astrophysics, University of Oxford, NAPL, Keble Road, OX2 6HT, UK*

¹⁵*CENTRA, Instituto Superior Tecnico, Lisbon, Portugal*

¹⁶*Physique Corpusculaire et Cosmologie, Collège de France,*

11 Place Marcelin Berthelot, 75231 Paris Cedex 05, France

¹⁷*School of Physics and Astronomy, University of Minnesota/Twin Cities, Minneapolis, MN 55455*

¹⁸*ENEA Centro Ricerche di Frascati, Via E. Fermi 45, 00044 Frascati, Italy*

¹⁹*University of Wales, Cardiff, UK, CF24 3YB*

²⁰*Departments of Physics and Astronomy, University of Toronto, Toronto M5S 3H8, Canada*

²¹*Department of Physics, University of California, Berkeley, CA 94720*

²²*Istituto Nazionale di Geofisica, Roma, Italy*

²³*Division of Physics, Lawrence Berkeley National Laboratory, Berkeley 94720, CA*

²⁴*Copernicus Astronomical Center, Warszawa, Poland*

Recent results from BOOMERANG-98 and MAXIMA-1, taken together with COBE-DMR, provide consistent and high signal-to-noise measurements of the CMB power spectrum at spherical harmonic multipole bands over $2 < \ell \lesssim 800$. Analysis of the combined data yields 68% (95%) confidence limits on the total density, $\Omega_{\text{tot}} \simeq 1.11 \pm 0.07$ (${}^{+0.13}_{-0.12}$), the baryon density, $\Omega_b h^2 \simeq 0.032^{+0.005}_{-0.004}$ (${}^{+0.009}_{-0.008}$), and the scalar spectral tilt, $n_s \simeq 1.01^{+0.09}_{-0.07}$ (${}^{+0.17}_{-0.14}$). These data are consistent with inflationary initial conditions for structure formation. Taken together with other cosmological observations, they imply the existence of both non-baryonic dark matter and dark energy in the universe.

PACS numbers: 98.80.-k; 98.70.Vc; 98.80.Es; 95.85.Bh

Measurements of the angular power spectrum, C_ℓ , of the Cosmic Microwave Background (CMB) have long been expected to enable precise determinations of cosmological parameters [1]. The CMB power spectrum depends on these parameters, as well as the scenario for the generation and growth of density fluctuations in the early universe. Evidence for structure in the CMB of the character predicted by adiabatic inflationary models has been mounting for the past decade and was convincingly detected in 1999 [2, 3, 4]. The recent BOOMERANG-98 (B98) [5] and MAXIMA-1 [6] CMB anisotropy data pro-

vide a significant improvement in the determination of C_ℓ . This letter jointly analyzes these two data sets, incorporating COBE-DMR [7] and other cosmological information to obtain further estimates of several cosmological parameters.

MAXIMA-1 and B98 have produced independent power spectra from patches of sky roughly 90° apart, on opposite sides of the galactic plane ([5, 6] and references therein). These data provide the first narrow-band detections of the power spectrum from $400 \lesssim \ell \lesssim 800$, where further acoustic peaks are expected in adiabatic models.

Each spectrum shows a well-defined peak at multipole $\ell \sim 200$, followed by a relatively flat region extending to the highest multipoles reported (Figure 1, top). These results have been interpreted as supporting the inflationary theory of structure formation with adiabatic initial conditions, and allow the first precise CMB measurements of other parameters such as the baryon density [8, 9, 10].

Comparison & Calibration. The B98 and MAXIMA-1 angular power spectra [12] are shown in the top panel of Fig. 1, along with some best-fit models. The B98 (MAXIMA-1) data cover $\ell = 25\text{--}625$ ($36\text{--}785$) with a resolution $\delta\ell = 50$ (75). The DMR data provide information at low ℓ . Each data set has a calibration uncertainty (20% for B98, 8% for MAXIMA-1, 1σ in C_ℓ) and a beam uncertainty (10% for B98, 5% for MAXIMA-1) that are not included in the errors plotted in Fig. 1. We take these uncertainties into account by allowing the overall amplitude (calibration) as well as an ℓ -dependent amplitude (beam) to vary for each spectrum, weighted by the distribution of errors around the nominal beam and calibration values.

We have combined the two data sets in the bottom panel of Fig. 1. We approximate the likelihood in the manner of [4, 11], treating the individual bandpowers as the parameters to be determined. The combined power spectrum requires an increase in the calibration by a factor 1.14 ± 0.10 for B98 and a decrease by 0.98 ± 0.08 for MAXIMA-1, along with a beam rescaling of 1.07 ± 0.09 for B98 and 0.99 ± 0.05 for MAXIMA-1.

We define a goodness-of-fit parameter, $\chi^2 \equiv -2 \ln \mathcal{L}$, in terms of the likelihood function, \mathcal{L} , which reduces to the usual χ^2 for a Gaussian. The data shown in the top panel of Fig. 1 have $\chi^2/\text{DOF} = 11.6/8$ with respect to the combined spectrum of the bottom panel (22 data points, 10 bandpowers and 2 beam rescalings and 2 calibration parameters give 8 degrees of freedom [DOF]) when DMR is not included, and a $\chi^2/\text{DOF} = 34/29$ with DMR. This indicates that the results are each consistent with a single underlying power spectrum.

Cosmological Parameters. We consider a subset of parameters describing a Friedmann-Robertson-Walker Universe with adiabatic initial conditions. The present-day density ρ_i of a component i is $\Omega_i = 8\pi G\rho_i/(3H_0^2)$ where $H_0 = 100h$ km/s/Mpc is the Hubble constant; thus $\Omega_i h^2$ is a physical density, independent of H_0 . We consider the density of baryons, Ω_b ; the density of cold dark matter (CDM), Ω_c ; the total density of matter, $\Omega_m = \Omega_c + \Omega_b$; the effective density of a cosmological constant, Ω_Λ ; and finally the total density $\Omega_{\text{tot}} = \Omega_m + \Omega_\Lambda$, ignoring other possible components. The initial spectrum of density perturbations is described by an amplitude factor, \mathcal{C}_{10} , multiplying the CMB spectrum, and the spectral tilt of scalar (density) perturbations, n_s (defined so the initial three-dimensional perturbation spectrum is $P(k) \propto k^{n_s}$). We also consider the optical depth to the epoch of reionization, τ_C . Our parameter space is thus

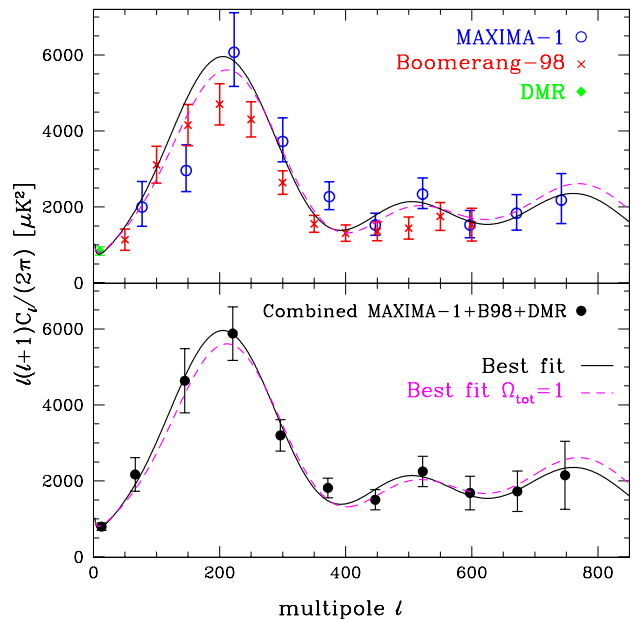


FIG. 1: CMB power spectra, $C_\ell = \ell(\ell + 1)C_\ell/2\pi$. Top: MAXIMA-1, B98 and COBE-DMR. Bottom: maximum-likelihood fit to the power in bands for the three spectra, marginalized over beam and calibration uncertainty. In both panels the curves show the best fit model in the joint parameter estimation with weak priors and the best fit with $\Omega_{\text{tot}} = 1$. These models have $\{\Omega_{\text{tot}}, \Omega_\Lambda, \Omega_b h^2, \Omega_c h^2, n_s, \tau_C\} = \{1.2, 0.5, 0.03, 0.12, 0.95, 0\}$, $\{1, 0.7, 0.03, 0.17, 0.975, 0\}$. They remain the best fits when the large scale structure prior [21] is added, and when the SN prior [22] is added the $\Omega_{\text{tot}} = 1$ model becomes the best fit in both cases.

$\{\Omega_{\text{tot}}, \Omega_\Lambda, \Omega_b h^2, \Omega_c h^2, n_s, \tau_C, \ln \mathcal{C}_{10}\}$ [13].

Because many of these parameters affect the spectrum in highly correlated (in some cases almost degenerate) ways, *limits on any one parameter are necessarily a function of the constraints, implicit and explicit, that one assumes for the other parameters.* Thus, all such limits must be understood in the context of the specific question that one asks of the data.

Inflation predicts $\Omega_{\text{tot}} = 1$. Fig. 1 shows that the data are consistent with this prediction: there exist $\Omega_{\text{tot}} = 1$ models that fit the data well with quite reasonable choices for all of the other parameters. Simultaneously maximizing the likelihood for all parameters at once gives $\Omega_{\text{tot}} = 1.2$. As is clear from the Figure, the global best-fit model and the best-fit flat model both fit the data with $\chi^2/\text{DOF} \lesssim 1$. Extracting quantitative conclusions from a simple χ^2 analysis is complicated by the fact that parameters are correlated with one another and are bounded by other cosmological observations. This issue will be explored elsewhere.

In this paper, we constrain parameters individually by marginalizing (integrating the posterior distribution) over all other parameters (including those describing uncertainty in the beam and calibration). We apply the techniques used on B97 [3], B98 [8] and MAXIMA-1 [9]

to the combined data. We calculate the likelihood of a suite of models given the DMR, MAXIMA-1, and B98 results, taking into account the correlations within each data set, as well as the non-Gaussianity of the likelihood functions [11, 15]. We use the median, 16% and 84% integrals as central and $\pm 1\sigma$ error estimates respectively. 95% limits are approximately twice the quoted errors.

The most likely value of each parameter calculated in this way will, in general, be different from that found by multi-dimensional maximization. Marginalization has the advantage of taking into account the likelihood structure over the entire space, weighted by the likelihood value and the volume of the parameter space. It has the disadvantage of allowing models whose validity we may doubt to influence the final result. Hence, it is crucial to restrict the range that each parameter may take on through the prudent use of “prior” constraints, and to test how the results change under a change of priors.

The finite range of each parameter that is included in our model database acts as a uniform (tophat) prior probability density [16]. We further restrict the analysis to the cosmologically interesting regime of $0.45 < h < 0.90$, age $t_0 > 10$ Gyr, and $\Omega_m > 0.1$; we refer to this combination as our “weak prior.” Without such restrictions the data sets allow pathological low-sound-speed models with strong positive curvature ($\Omega_k < 0$), very high baryon density, and very young ages. Parameter degeneracies allow such models to contribute to or dominate the likelihood [8, 17]. The results presented here were checked using the methods of [3, 9] and found to be in good agreement [18].

Results are shown in Table I. The combined data yield parameters consistent with those derived individually: the curvature is close to flat, the spectral index is close to unity, and the baryon density is about 2σ above (with respect to our CMB confidence limits) the favored Big-Bang nucleosynthesis (BBN) value of $\Omega_b h^2 = 0.019 \pm 0.002$ [19]. This high value suppresses the second acoustic peak relative to standard CDM models.

In Figure 2 we plot likelihoods for several parameters using the two data sets independently [18], and for the joint analysis. We also plot likelihood contours, showing how the CMB primarily restricts $\Omega_{\text{tot}} = \Omega_m + \Omega_\Lambda$. Projecting this figure onto either axis gives the likelihood for the quantities separately. This indicates the danger of individual parameter estimates in the presence of strong correlations: for example, neither Ω_m nor Ω_Λ are well-determined individually by the CMB data alone.

We have also investigated the effects of applying various prior probabilities [8]. Overall, the results from the combined data are somewhat less dependent on the priors than either individually. We find that any prior restriction that does not seriously contradict the locus of good-fitting models has very little effect on the parameter estimates. Incorporating previous CMB data [4, 8, 11] has very little effect. Restricting the Hubble constant to

TABLE I: Parameter estimates from the two data sets [18], and the combined data, using the weak prior ($0.45 < h < 0.90$, $t_0 > 10$ Gyr, $\Omega_m > 0.1$). Below the line, we restrict the parameter space to $\Omega_{\text{tot}} = 1$ and add other cosmological information. Central values and 1σ limits are found from the 50%, 16% and 84% integrals of the marginalized likelihood. τ_C and Ω_Λ are not constrained by the data.

	Ω_{tot}	$\Omega_b h^2$	n_s	$\Omega_c h^2$
B98+DMR	$1.15^{+0.10}_{-0.09}$	$0.036^{+0.006}_{-0.005}$	$1.04^{+0.10}_{-0.09}$	$0.24^{+0.08}_{-0.09}$
MAXIMA-1+DMR	$1.01^{+0.09}_{-0.09}$	$0.031^{+0.007}_{-0.006}$	$1.06^{+0.10}_{-0.09}$	$0.18^{+0.07}_{-0.06}$
B98+MAXIMA-1+DMR	$1.11^{+0.07}_{-0.07}$	$0.032^{+0.005}_{-0.005}$	$1.01^{+0.09}_{-0.08}$	$0.14^{+0.06}_{-0.05}$
+($\Omega_{\text{tot}} = 1$)	1	$0.030^{+0.004}_{-0.004}$	$0.99^{+0.07}_{-0.06}$	$0.19^{+0.07}_{-0.06}$
CMB+LSS	$1.11^{+0.05}_{-0.05}$	$0.032^{+0.004}_{-0.004}$	$1.00^{+0.09}_{-0.06}$	$0.13^{+0.02}_{-0.01}$
CMB+SNIa	$1.09^{+0.06}_{-0.05}$	$0.032^{+0.005}_{-0.005}$	$1.00^{+0.09}_{-0.08}$	$0.10^{+0.04}_{-0.04}$
CMB+LSS+SNIa	$1.06^{+0.04}_{-0.04}$	$0.033^{+0.005}_{-0.004}$	$1.03^{+0.09}_{-0.07}$	$0.14^{+0.03}_{-0.02}$

$h = 0.71 \pm 0.08$ [20] does push the curvature closer to flat: $\Omega_{\text{tot}} = 1.05^{+0.04}_{-0.04}$. A strong BBN prior ($\Omega_b h^2 = 0.019 \pm 0.002$ [19]), disfavored by the current CMB data, pushes other quantities to compensate, such as $n_s = 0.89 \pm 0.06$.

We determine parameters which are functions of those used to explicitly define our parameter space by calculating their means and variances over the full probability distribution. We find $h = 0.57 \pm 0.11$ and age $t_0 = 14.6 \pm 2.0$ Gyr. Restricting to $\Omega_{\text{tot}} = 1$ gives $h = 0.75 \pm 0.10$, $t_0 = 11.8 \pm 0.8$ Gyr. To illustrate the effect of the priors alone, we give the following limits without including CMB data: $h = 0.63 \pm 0.11$, $t_0 = 12.3 \pm 1.9$ Gyr.

The combined data improve the constraint on the matter density and cosmological constant, but we caution that these results are influenced by the weak prior alone (e.g., $\Omega_c h^2 = 0.18^{+0.11}_{-0.10}$ without CMB data). However, prior information from other cosmological data tightens these limits considerably. We consider the constraints on the power spectrum from observations of large-scale-structure (LSS) [21] and from observations of distant Supernova Ia (SNIa) [22] as in the bottom of Fig. 2. CMB+LSS gives $(\Omega_m, \Omega_\Lambda) = (0.49 \pm 0.13, 0.63^{+0.08}_{-0.09})$; (note that Ω_m is a function of the explicit database parameters, and thus its confidence limits are calculated as discussed above) CMB+SNIa gives $(0.35 \pm 0.07, 0.75^{+0.06}_{-0.07})$; combining all three gives $(0.37 \pm 0.07, 0.71 \pm 0.05)$ for CMB+LSS+SNIa. We note that the combination of CMB+LSS is about as restrictive as—and compatible with—the combination of CMB+SNIa.

Conclusions. The MAXIMA-1 and B98 data are consistent with one another over the range of overlapping coverage in ℓ . The consistency between the two data sets, obtained by different experiments using different observation strategies on different parts of the sky, eliminates many sources of systematic error as cause for concern.

These data, together with those of COBE-DMR, sup-

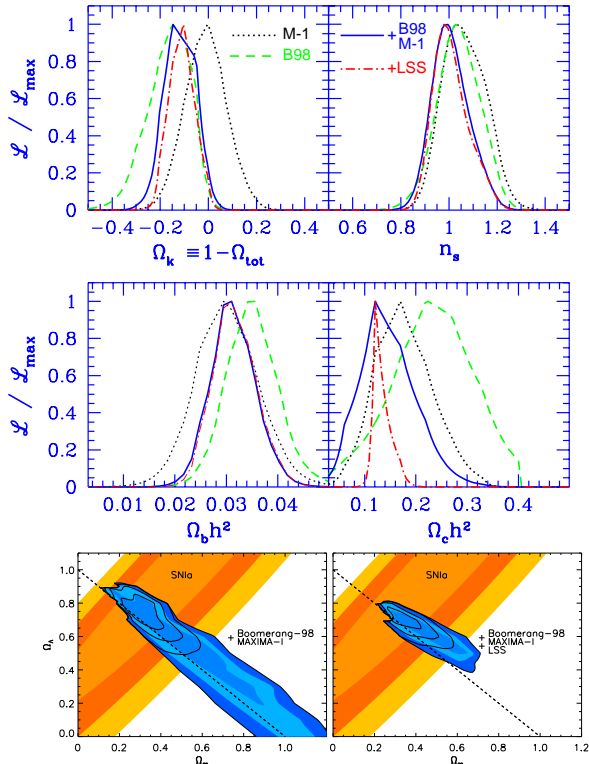


FIG. 2: Likelihood functions calculated using the weak prior. Top: likelihoods from DMR+B98, DMR+MAXIMA-1(M-1) [18], DMR+MAXIMA-1+B98 and DMR+MAXIMA-1+B98+LSS (LSS is the large-scale structure prior [21]). Bottom: the likelihood in $(\Omega_m, \Omega_\Lambda)$. Shaded contours nearly parallel to $\Omega_m + \Omega_\Lambda = 1$ are one-, two-, and three-sigma limits, defined as the equivalent likelihood ratio for a two-dimensional Gaussian distribution, from DMR+B98+MAXIMA-1 with weak priors (left) and DMR+B98+MAXIMA-1+LSS (right). Contours labeled “SNIa” are from high-redshift supernovae observations [22], and the final heavy set of contours are constraints from the product of the two distributions.

port the chief predictions of the inflation paradigm, that the geometry of the universe is flat, and that the initial density perturbations are scale-invariant, and with the corollary that the density of mass-energy in the universe is dominated by a form other than ordinary matter. Simple models of topological defects driving structure formation are difficult to reconcile with the CMB data [23]. These conclusions are considerably strengthened by the inclusions of other cosmological data, such as measurements of the Hubble constant, the amplitude and shape of the matter power spectrum, and the accelerating expansion rate indicated by observations of distant Supernovae.

Marginalization of the combined data over all other parameters yields a value for the physical density of baryons of $\Omega_b h^2 = 0.032 \pm 0.005$, (0.030 ± 0.004 if $\Omega_{\text{tot}} = 1$). These results are each more than 2σ higher than the values determined from the relative abundance of light elements

and the theory of BBN [19].

The data analyzed here present only a suggestion of the expected second acoustic peak in the CMB power spectrum. A detailed mapping of that ℓ region with higher signal-to-noise may yield more convincing detections of acoustic oscillations, providing yet more evidence for the adiabatic inflationary paradigm and measurements of the cosmological parameters. Already, the combined data begin to limit the CDM density, driven by the B98 constraints on the first peak and the MAXIMA-1 constraints over $650 \lesssim \ell \lesssim 800$. Both teams are analyzing additional data which may significantly reduce the errors in the region of the power spectrum where further peaks are expected.

The MAXIMA-1 and B98 teams acknowledge support from the NSF through the Center for Particle Astrophysics at UC Berkeley, the NSF Office of Polar Programs, the NSF KDI program, from NASA, and from the DoE through NERSC in the USA; PPARC in the UK; and Programma Nazionale Ricerche in Antartide, Agenzia Spaziale Italiana and University of Rome La Sapienza in Italy. We thank the High-Z SN team and Saurabh Jha and Peter Garnavich in particular for supplying SNIa likelihoods and for useful conversations.

- [1] For example, G. Jungman *et al.*, Phys. Rev. Lett. **76**, 1007 (1996); G. Jungman *et al.*, Phys. Rev. D **54**, 1332 (1996); J.R. Bond, G. Efstathiou & M. Tegmark, Mon. Not. R. Astron. Soc. **291**, L33 (1997) and references therein.
- [2] A.D. Miller *et al.*, Astrophys. J. **524**, L1 (1999) astro-ph/9906421; P. Mauskopf *et al.*, Astrophys. J. **536**, L63-L66 (2000), astro-ph/9911444.
- [3] A. Melchiorri *et al.*, Astrophys. J. **536**, (2000), L59-L62 astro-ph/9911445.
- [4] S. Dodelson & L. Knox, Phys. Rev. Lett. **84**, 3523 (2000), astro-ph/9909454.
- [5] P. de Bernardis *et al.*, Nature (London) **404**, 995 (2000), astro-ph/0004404.
- [6] S. Hanany *et al.*, Astrophys. J. **545**, L5 (2000), astro-ph/0005123.
- [7] C. Bennett *et al.*, Astrophys. J. **464**, L1 (1996).
- [8] A.E. Lange *et al.*, Phys. Rev. D submitted (2000), astro-ph/0005004
- [9] A. Balbi *et al.*, Astrophys. J. **545**, L1 (2000), astro-ph/0005124.
- [10] M. White, D. Scott & E. Pierpaoli, Astrophys. J. Lett., submitted (2000), astro-ph/0004385; M. Tegmark & M. Zaldarriaga, Phys. Rev. Lett. **85**, 2240 (2000), astro-ph/0004393.
- [11] J.R. Bond, A.H. Jaffe & L. Knox, Astrophys. J. **533**, 19 (2000); astro-ph/9808264.
- [12] The individual bandpowers will be available at <http://cfpa.berkeley.edu/maxima>, <http://oberon.roma1.infn.it/boomerang>, and <http://www.physics.ucsb.edu/~boomerang/>.

- [13] We ignore several other parameters not constrained by these data. The quintessence equation-of-state [14] is largely degenerate with Ω_Λ and Ω_m ; the neutrino density has only a tiny effect on C_ℓ in the regime probed here; the gravity-wave amplitude awaits polarization measurements before it can be disentangled from the scalar amplitude.
- [14] For example, M.S. Turner in *Proceedings of Physics in Collision*, edited by M. Campbell & T.M. Wells (World Scientific, NJ, 2000), astro-ph/9912211; P. Brax, J. Martin & A. Riazuelo, Phys. Rev. D **62**, 103505 (2000), astro-ph/0005428.
- [15] J.R. Bond, A.H. Jaffe & L. Knox, Phys. Rev. D **57**, 2117 (1998), astro-ph/9708203.
- [16] The amplitude C_{10} is a continuous variable. The rest are discretized over: $0.1 \leq \Omega_{\text{tot}} \leq 1.5$; $0.0031 \leq \Omega_b h^2 \leq 0.2$; $0.03 \leq \Omega_c h^2 \leq 0.8$; $0 \leq \Omega_\Lambda \leq 1.1$; $0 \leq \tau_C \leq 0.5$; $0.5 \leq n_s \leq 1.5$. A full discussion of the effect of limits and other priors on parameter determinations is in [8].
- [17] G. Efstathiou & J.R. Bond, Mon. Not. R. Astron. Soc. **304**, 75 (1999).
- [18] The small differences between the MAXIMA-1 results here and in [9] can be ascribed to differences in the parameter ranges and database gridding; restricting the parameter limits gives more consistent results and provides a check on the methods.
- [19] K.A. Olive, G. Steigman & T.P. Walker, Phys. Rep. **333-334**, 389 (2000), astro-ph/9905320; S. Burles, K. Nollett, J. Truran & M.S. Turner, Phys. Rev. Lett. **82**, 4176 (1999), astro-ph/9901157; D. Tytler, J.M. O'Meara, N. Suzuki & D. Lubin, Physica Scripta submitted, astro-ph/0001318 (2000); S. Burles, K. Nollett & M.S. Turner, Phys. Rev. D (2001), astro-ph/0008495, gives a slightly higher value of $\Omega_b h^2 = 0.020 \pm 0.002$.
- [20] W.L. Freedman, Phys. Rep. **333-334**, 13 (2000), astro-ph/9909076; J.R. Mould *et al.*, Astrophys. J. **529**, 786 (2000); W.L. Freedman *et al.*, astro-ph/0012376 (2000).
- [21] The LSS prior constrains the amplitude using cluster abundances, $\sigma_8 \Omega_m^{0.56} = 0.55_{-0.02, -0.08}^{+0.02, +0.11}$, distributed as a Gaussian (first error) smeared by a uniform (tophat) distribution (second error). [See also, e.g., J.P. Henry, Astrophys. J. **534** 565 (2000) which breaks this degeneracy somewhat.] We constrain the shape of the power spectrum via $\Gamma + (n_s - 1)/2 = 0.22_{-0.04, -0.07}^{+0.07, +0.08}$, where $\Gamma \approx \Omega_m h e^{-(\Omega_B(1+\Omega_m^{-1}(2h)^{1/2})-0.06)}$. More details are in [8] and J.R. Bond & A.H. Jaffe, Phil. Trans. R. Soc. London **357**, 57 (1999), astro-ph/9809043.
- [22] A.G. Riess *et al.*, Astron. J. **116**, 1009 (1998); S. Perlmutter *et al.*, Astrophys. J. **517**, 565 (1999).
- [23] F.R. Bouchet, P. Peter, A. Riazuelo, M. Sakellariadou, Phys. Rev. Lett. submitted (2000), astro-ph/0005022. C. Contaldi, Phys. Rev. Lett. submitted, astro-ph/0005115.